TOP FLANGE FAILURE MODES FOR CALIFORNIA WIDE FLANGE GIRDER USING REBAR AND WELDED WIRE DETAILS

Alban Gjongecaj, MS, PE, Burne Engineering, El Dorado Hills, CA
Eric Matsumoto, PhD, PE, Dept. of Civil Engineering, California State University Sacramento, CA

ABSTRACT

In an effort to advance Accelerated Bridge Construction (ABC) practices in California, top flange failure modes were investigated for the newly developed California Wide Flange Girder (WFG) using precast deck panels (PDP) supported by polystyrene camber strips.

Both sides of the top flange for two WFG specimens were tested to failure by loading the edge of the flange with a line load to simulate loading from a PDP during construction. The specimens used different top flange reinforcement details, namely, rebar and welded wire reinforcement (WWR). The location of the center of bearing was varied for each test to examine flange behavior, failure mode, failure location, and capacity.

The two rebar specimen flanges exhibited a ductile flexural failure and a flexural-shear failure (with significant ductility), respectively; both WWR specimens demonstrated brittle shear failures with limited ductility.

Failure loads and failure modes suggest that flexural cracking of the top flange is not expected under typical construction loads. Permissible line loads during construction are derived from test results and recommendations are presented for improved details, including bearing location of PDPs on top flanges, size of supporting camber strip, and minimum side cover of the top flange reinforcement.

Keywords: Accelerated Bridge Construction, ~~Research~~Wide Flange Girder, ~~Design-Build~~Precast Deck Panel, Research

INTRODUCTION

In the early 2000's the California Department of Transportation (Caltrans) began developing a new pretensioned girder in coordination with the bridge industry. The new California Wide Flange Girder (WFG) was first introduced in California in 2007 at the 14th Annual Caltrans/PCMAC Bridge SeminarTadros, M. K., "New Developments in Long Span Precast Girder Technology", 14th Annual Caltrans/PCMAC Bridge Seminar Proceedings, Sacramento, CA, 2007, at which time it was aptly called a Super Girder. The girder shape was based in part on the Nebraska (NU) I-Girder, which was successfully used for over 20 years priorGeren, L. K., Tadros, M. K., "The NU Precast/Prestressed I-Girders Series", PCI Journal, V. 39, No. 3, May-June 1994. By 2009, a family of standard pretensioned and post-tensioned WFG shapes was developed and presented at the 16th Annual Caltrans/PCMAC Bridge SeminarMa, J., "The New Wide-Flange Girder Family in California: Benefits and Capabilities", 16th Annual Caltrans/PCMAC Bridge Seminar Proceedings, Sacramento, CA, 2009. This new girder shape was evaluated to be more efficient and span larger distances; however, future innovations were outlined as necessary to further develop and implement this girder, among which was its use in conjunction with partial-depth precast deck panels (PDP)Ma, J., "The New Wide-Flange Girder Family in California: Benefits and Capabilities", 16th Annual Caltrans/PCMAC Bridge Seminar Proceedings, Sacramento, CA, 2009. As of 2012, the WFG was one of the standard precast-prestressed shapes available to designers in California through Caltrans Bridge Design AidsCaltrans, "Bridge Design Aids", California Department of Transportation, Sacramento, CA, 2012.

Recent considerations of using partial-depth PDPs with the WFG to further implement Accelerated Bridge Construction (ABC) practices in California led Caltrans to question to possibility of local cracking and potential failure of the top flange of the WFG when used in conjunction with partial-depth PDPs. To address these concerns during early stages of a project, Con-Fab California Corporation (Con-Fab) conducted a limited verification test to examine potential top flange cracking due to PDP self-weight and an estimate of a topping slab and construction live loads. For verification, ~~Con-Fab fabricated~~ two WFG stub specimens were fabricated, 8'-6" long by 4' tall, in early March of 2014. The specimens were identical in cross section but used different top flange reinforcement, namely, rebar and welded wire reinforcement (WWR). The specimens were placed side by side and loaded near the edge of the flanges using three slabs. Loading included the following:

i. 8 ½" slab, representing the self-weight of the PDP (3 ½" thick) and topping slab (5" thick)

ii. 4 ¼" slab, representing a 50 psf construction live load (approximate)

iii. 4 ¼" slab, representing the additional load due to dead and live load factors of 1.2 and 1.6, respectively

The objective of the Con-Fab test was to verify the ability of the WFG top flange to support design dead and construction live loads non-compositely, without cracking or other damage. In this test, the specimens were spaced 12' apart and with no cross slope. This test lasted approximately 45 minutes. A second test, over 4 days, was conducted in which one of the specimens was raised 1’, producing an 8% cross slope. The total line load on each girder top flange was 0.95 klf, corresponding to a total load of 7.6 kips. A 2” square foam camber strip was used to support the PDPs in all cases. Draft Caltrans XS sheets specify camber strips (though not foam) can be a rectangle or square, varying from 1” x 2” to 2” x 4”XS01-180-1e, “Precast Concrete Deck Panel Polystyrene Support System”, Draft XS Sheets, State of California Department of Transportation, CA, 2013.

The specimens withstood the applied loads without cracking or observable damage. However, important questions remained, such as “What load would actually cause initial cracking of the flange?”, “What crack type would form and what location?”, “What would be the failure load and mode?”, and “What differences in response might occur due to the different detailing and PDP bearing locations used?” Investigation of these issues were considered to potentially improve detailing of the WFG and PDP XS Sheets and establish design loads for construction. In coordination with Caltrans, California State University, Sacramento (CSUS) requested that Con-Fab donate the undamaged specimens for testing to failure at the Sacramento State Structural Engineering Research Laboratory. ~~Con-Fab graciously donated and shipped the two specimens to CSUS for testing to failure.~~

RESEARCH OBJECTIVE

The primary objectives of the research were to:

1) determine the failure modes of the WFG top flange using rebar and WWR details, including the effect of different bearing locations for PDPs supported by polystyrene camber strips and loads corresponding to key stages of response, including initial flexural cracking;
2) establish improved details for the Caltrans WFG and PDP XS sheets; and
3) establish conservative design line loads to prevent damage to WFGs during construction.

SPECIMEN FABRICATION

The two specimens were fabricated in the ~~Con-Fab~~ precast yard in Lathrop, CA, in March of 2014. Figure 1 and Figure 2 show the reinforcement for each specimen, including the difference in the top flange reinforcement. The rebar specimen used #4’s @ 12” in the transverse direction (primary flexural reinforcement direction) with (6) #3’s longitudinally, whereas the WWR specimen used D20 @ 12” transversely with (6) W8 longitudinally. Although a D20 nominally provides the same area of reinforcement, the material properties differ from rebar in terms of yield and ultimate strengths. The web and bottom flange reinforcement was identical for both specimens [Figure 3]. It should be noted that the top flange transverse reinforcement was constructed with a 2” cover to the side face of the girder, which is ~~less~~ greater than the 1½” specified in the current Caltrans draft XS sheetsXS01-180-1e, “Precast Concrete Deck Panel Polystyrene Support System”, Draft XS Sheets, State of California Department of Transportation, CA, 2013. This was done to increase the severity of the initial ~~Con-Fab~~ test. Each specimen had four through holes on the bottom flanges; this allowed the specimen to be tied down during testing at Sacramento State.

A self-consolidating concrete (SCC) mix design was used for both specimens. This was a 9.5 sack mix, with 25% of the Portland cement replaced by fly ash. The sieve analysis and proportioning of this mix are shown in Figure 4. Research suggests that, in general, SCC mixes exhibit lower modulus of elasticity and greater drying shrinkage. After casting, each specimen was steam cured for approximately 18 hours. The mix design and curing method are representative of pretensioned bridge girders in California.

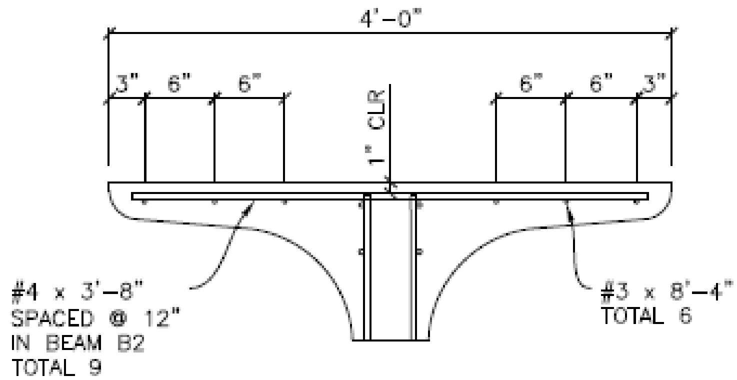

Figure *1* - Top Flange Detailing for Rebar Specimen*Koch, B. R., "Wide Flange Test For Capacity To Support Deck Panels", Construction Drawings, ConFab California Corporation, Lathrop, CA, 2014*

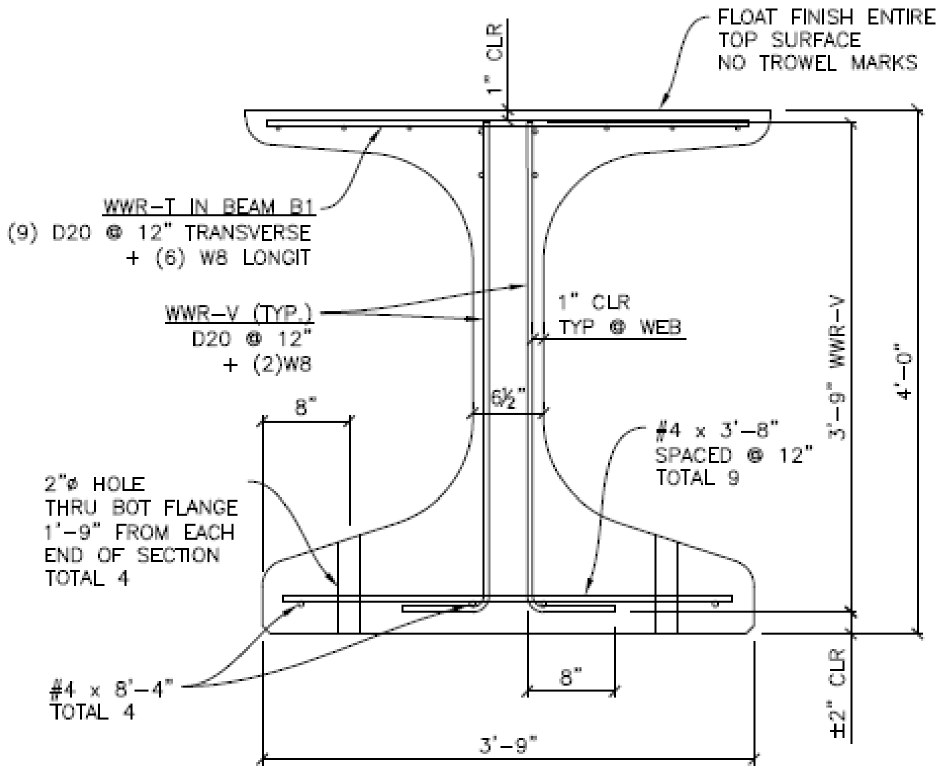

Figure 2 - Typical Section and Top Flange Detailing for WWR Specimen*Koch, B. R., "Wide Flange Test For Capacity To Support Deck Panels", Construction Drawings, ConFab California Corporation, Lathrop, CA, 2014*

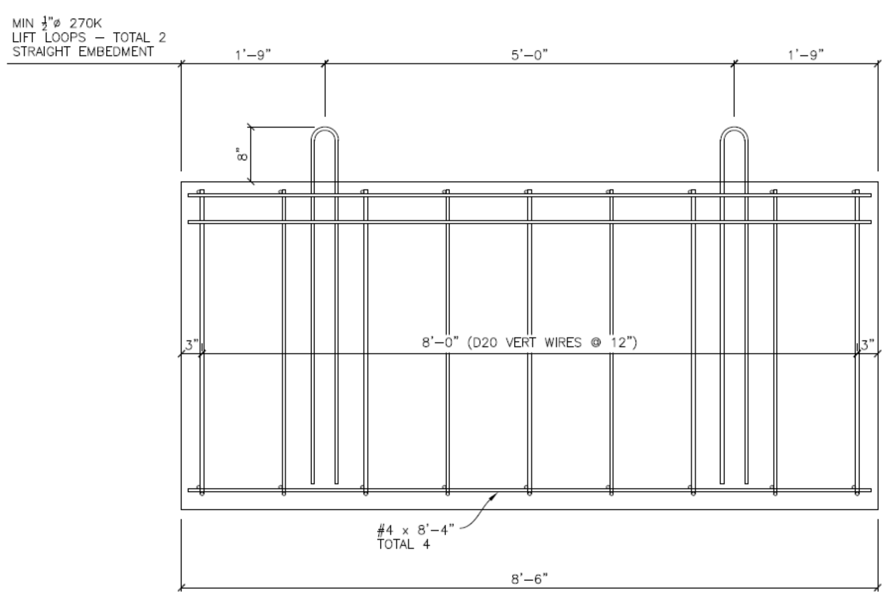

Figure 3 - Typical Elevation of Specimens Showing Web Reinforcement*Koch, B. R., "Wide Flange Test For Capacity To Support Deck Panels", Construction Drawings, ConFab California Corporation, Lathrop, CA, 2014*

SIEVE ANALYSIS (% Passing)												
Sieve	1 1/2"	1"	3/4"	1/2"	3/8"	#4	#8	#16	#30	#50	#100	#200
	37 1/2	25	19	12.5	9.5	4.75	2.36	1.18	600	300	150	75
1/2" x 3/8" Crushed	100	100	100	88	38	4	2	1	0	0	0	0
3/8"Pea Gravel	100	100	100	100	91.0	17.0	4.0	2.0	0.0	0.0	0.0	0.0
Combined Rock	100.0	100.0	100.0	94.0	64.5	10.5	3.0	1.5	0.0	0.0	0.0	0.0
Conc. Sand	100	100	100	100	100	100	88	61	41	22	8	1.9
Total Combined	100.0	100.0	100.0	97.0	82.1	54.8	45.1	31.0	20.3	10.9	4.0	0.9
Caltrans	100	100.0	100.0	90-100	55-86	45-63	35-49	25-37	15-25	5-15	1-8	0-4

Cement Content: 9.5 sacks / CY (total cementitious materials)

Specified Strength:	6000 - 6500	psi at release
	8000	psi at 28-days

Flow:	23" ± 3"

Entrained Air: none
Water/Cement Ratio: 0.30
Slump: 0.5" - 2" Before Superplasticizer

Admixtures:					
Plasticizer ADVA Cast 575	Dosage:	7.25	oz/tcwt=	65	oz/CY*
V-MAR 3 (If Needed)	Dosage:	2	oz/tcwt=	18	oz/CY*
Recover (If needed)	Dosage:	2	oz/tcwt=	18	oz/CY

* Add/reduce dosage to meet flow requirements
All Admixtures are Manufactured by WR GRACE

MIXTURE PROPORTIONING					
MATERIAL	SPECIFIC	S.S.D.	Abs. VOL	DENSITY	SOURCE
1/2" x 3/8" Crushed	2.650	723	4.37	165.36	KRC-Vernalis , Tracy, CA. SMARA Mine ID# 91-39-0029
3/8" x #4 Crushed	2.630	723	4.41	164.11	
Concrete Sand	2.640	1,420	8.62	164.74	
Hanson Pronto, T-II Cement	3.15	671	3.41	196.56	Lehigh, Cupertino, CA
Flyash, Type "F"	2.39	224	1.5	149.14	Headwaters, Stocton, CA
Water	1	268	4.29	62.40	
Air (@1.5%)			0.40		
TOTAL		4,029	27.00	149.22	

Figure *4* - SCC Mix Design Used for Both Specimens[*Koch, B. R., "Wide Flange Test For Capacity To Support Deck Panels", Construction Drawings, ConFab California Corporation, Lathrop, CA, 2014*]

TEST PROGRAM

The CSUS research team determined a testing approach that would allow two tests to be conducted, one on each side of the top flange of a specimen. In order to simulate loading from the PDP, each flange was to be loaded quasi-statically to failure with a line load along the edge of the top flange. Based on collaboration with the Industry Advisory Committee, it was decided that the baseline (control) test for each specimen (Rebar and WWR) would use a center of bearing location 1½" from the edge of the top flange. This distance represents the sum of three items [see Figure 5 and Figure 6]:

1) ½": minimum edge distance between the polystyrene camber strip and the edge of the top flange
2) ½": half of the minimum width of the smallest (1") camber strip for center of bearing
3) ½": extra cover used for top flange reinforcement when specimens were fabricated

It should be noted that, for item ½”: minimum edge distance between the polystyrene camber strip and the edge of the top flange, the Caltrans draft XS sheets for PDPsXS01-180-1e, “Precast Concrete Deck Panel Polystyrene Support System”, Draft XS Sheets, State of California Department of Transportation, CA, 2013 indicate that the minimum edge distance for a camber strip is 1/8”; however, it was agreed that a more realistic distance to use for the control test would be ½”. This gave a total distance of 1.5” to center of bearing, in view of a possible update to XS sheets that would reflect more reasonable field practice. Even with the 1.5” distance, the center of bearing was still located beyond the (premature) bar termination used in the specimens, as shown in shown Figure 5, thereby allowing investigation of a poor detail.

Based on the results from the first test for each specimen, the research team and Industry Advisory Committee agreed to a revised center of bearing location for the second flange test. For the rebar specimen, it was decided to move the load 1” further toward the web to investigate a slightly more severe condition of shear, as well as for some measure of repeatability. For the WWR specimen, the 1.5” camber strip was placed flush with the edge of the top flange (i.e., moved ¾” closer to the edge). This used the most severe edge distance location, investigating the possibility of failure of the extreme edge of the top flange as well as providing some measure of repeatability.

The convention used to identify each test was a letter followed by a number. The letter represents the top flange detail (R=Rebar, W=WWR), the number represents the distance from the edge of the flange to the center of bearing of the load. The test matrix is shown in Table 1 below. The loading schematic for the Rebar and WWR tests is shown in Figure 5 and Figure 6, respectively.

Table 1 - Test Matrix

Specimen	**Test 1**		**Test 2**	
Rebar	R 1.5 R1.5A *	1”x1” Camber Strip w/ 1” Edge Distance; 1.5” center of bearing	R 2.5	1 ½”x1 ¼” Camber Strip w/ 1 ¾” Edge Distance; 2.5” center of bearing
WWR	W 1.5	1 ½”x1 ¼” Camber Strip w/ ¾” Edge Distance; 1.5” center of bearing	W 0.75	1 ½”x1 ¼” Camber Strip w/ 0” Edge Distance 0.75” center of bearing

*Due to test set up issues test R1.5 was not taken to failure, after adjusting the setup the test was repeated (R 1.5A) and the specimen was taken to failure

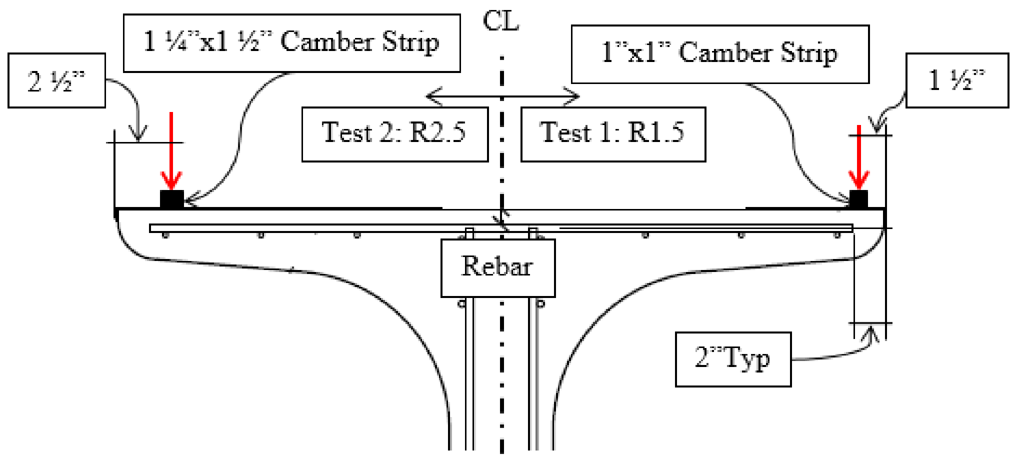

Figure 5 - Loading Schematic for Rebar Specimen

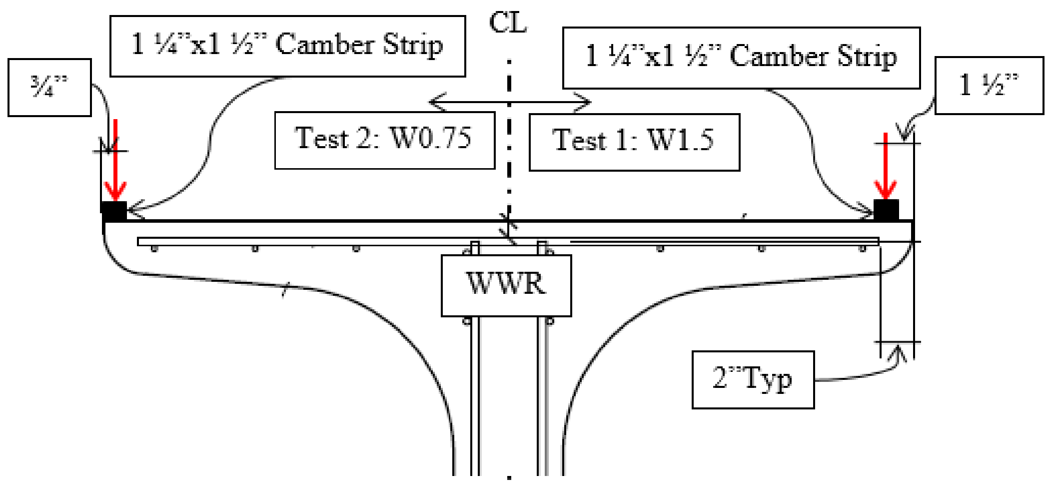

Figure 6 - Loading Schematic for WWR Specimen

TEST SETUP

The testing was conducted in the loading cell in the Structural Engineering Research Laboratory. Figure 7 shows a conceptual isometric view of the test setup in the design phase, and the actual test setup is shown in Figure 8.

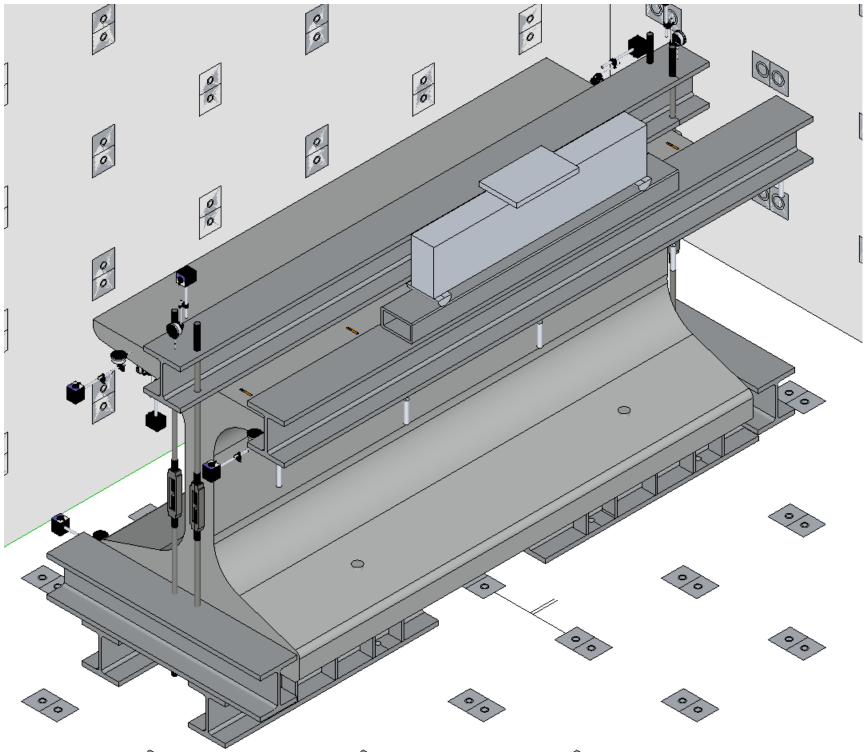

Figure 7 - Conceptual Isometric View of Test Setup

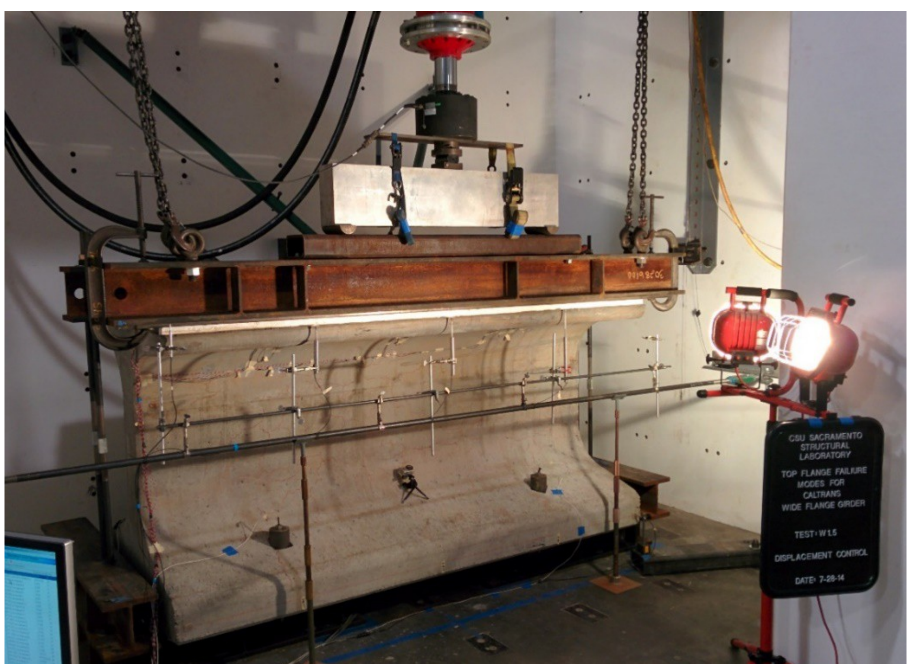

Figure 8 - Actual Configuration of Test Setup

The load was applied with a 100-kip hydraulic actuator. In order to spread the load as uniformly as possible along the top flange, a series of spreader beams were used. Initially the loading beam bore directly onto the foam camber strip. However, after the camber strip was fully compressed, the loading beam started bearing further on the specimen during test R1.5. This was corrected by clamping a steel bar, 1½” wide by ¾” tall, to the bottom of the loading beam over the camber strip. The steel bar was used for all other tests, including R1.5A. The width of the camber strip was also increase with the inclusion of the steel bar. The total height from the bottom of the actuator to the top surface of the specimen was 25¾”, which resulted in a 1:2 slope for the load distribution. The configuration of the loading setup is shown in Figure 9 below. For a detailed description of the various elements of the test setup and instrumentation used, see Reference Gjongecaj, A., “Top Flange Failure Modes for California Wide Flange Girder using Rebar and Welded Wire Details”, Thesis, California State University, Sacramento, CA, 2014.

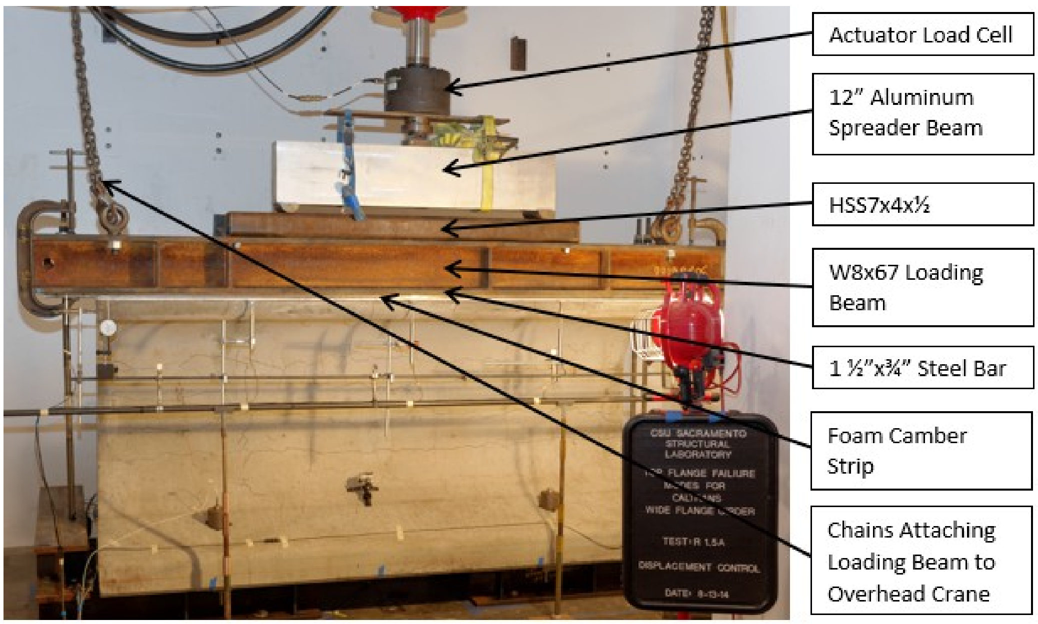

Figure 9 - Loading Configuration

The tests were conducted quasi-statically using a displacement control loading protocol, so that the loading rate was based on the actuator displacement rate. The actual deflection of the flange was measured by LVDTs. The tests were conducted with a smaller displacement rate at the start, but the rate was typically increased after the specimen cracked and the steel yielded to complete testing in an acceptable timeframe, as shown in Table 2. Changes in loading rate occurred when loading was paused (5 kip intervals). The load was generally well distributed along the length of flange, verified by the uniform flexural cracks on the top face of the specimens and the appearance of the cracks at the same time throughout the length. In addition, the crushing along the bottom face of the flange was generally uniform.

Table 2 - Summary of Loading Rates for All Tests

Test	Loading Rate (in/min)	Loading Range (kips)
R1.5	0.01	Start – End
W1.5	0.01	Start – 15.0

	0.02	15.0 – 25.0
	0.05	25.0 – 35.0
	0.1	35.0 - End
R2.5	0.05	Start – 35.0
	0.1	35.0 – End
R1.5A	0.05	Start – End
W0.75	0.05	Start - End

PRETEST PREDICTIONS

Two main methods were used to predict the response of the specimen under loading: idealized cantilever model and two-dimensional (2-D) frame model. The idealized cantilever model analyzed the flange only; the flange to web connection was considered as fixed and the increased deflection from the specimen rotating was ignored. This model was used to generate the load predictions. A 2-D frame model was used for the deflection predictions, which was based on a modified cantilever model to include the rotation of the web. The 2-D frame model analyzed the entire cross-section of the specimen, taking into account overall frame action of the specimen, including rotation at the flange-web joint. Both analytical models used a one-foot section of the specimen and ignored three-dimensional effects. The idealized cantilever model is described in detail in reference Gjongecaj, A., "Top Flange Failure Modes for California Wide Flange Girder using Rebar and Welded Wire Details", Thesis, California State University, Sacramento, CA, 2014; the 2-D frame model is beyond the scope of this paper. The material properties used for predictions were generated from testing, assumptions, and conventional industry values.

The idealized cantilever model was analyzed by treating the flange as a cantilevered beam with a varying cross-section along its length, fixed at the face of the web. Transformed section properties were used. For all cases, it was assumed that the flexural reinforcement would be engaged and developed; therefore, localized failure of the flange tip was ignored. The material properties (concrete, rebar, and WWR) used in the predictions were based on material tests.

Predictions of load were generated for the following stages of response: concrete cracking in flexure, flexural yielding of primary steel reinforcement, and ultimate flexural failure due to concrete crushing. In addition, shear failure was ~~considered using the Modified Compression Field Theory (MCFT) as described in~~ addressed using Appendix B of AASHTO LRFD Bridge Design SpecificationsAASHTO, "AASHTO LRFD Bridge Design Specifications, Customary U.S. Units, 6th Edition", American Association of State Highway and Transportation Officials, DC, 2012~~.~~, which is based on the Modified Compression Field Theory (MCFT). This is more accurate than the general procedure of Art. 5.8.3.4.2. ~~The calculated concrete strain values at failure exceed the range of values in the tables; therefore, linear interpolation was used to extrapolate the values of β and θ.~~

CONCRETE PROPERTIES AND TESTING

When the specimens were fabricated, cylinders were cast for each specimen. However, the cylinders were moist cured at ~~Con-Fab~~precast yard and at Sacramento State, while the specimens were kept outdoor in the ~~Con-Fab~~precast yard and the location at Sacramento State varied. Due to this uncertainty the Division of Engineering Services at Caltrans assisted in coring the specimens. Four cylinders (3x6), two from each end, were cored from each specimen.

Compression and split cylinder tests were performed. Compressive strength (f'_c) and tensile strength (f_{ts}) were obtained for each specimen. For the Rebar specimen cores, two cylinders were tested in compression, one in tension, and one was not used since it was damaged in a trial test. For the WWR specimen cores, two were tested in compression and two in tension.

Based on NevilleNeville, A. M., "Properties of Concrete", Fourth Edition, Pearson Education Inc., Essex, England, 2000, the tensile strength of 4x8 and 3x6 cylinders is smaller than that of standard 6x12 cylinders by a factor of approximately 0.87. Neville also indicates that the modulus of rupture, f_r, is approximately 1.5 times that of the split cylinder tensile strength for a 6x12 cylinder. Similar conclusions were reached by othersWight, J. K., MacGregor, J. G., "Reinforced Concrete Mechanics and Design", Sixth Edition, Pearson Education Inc., Upper Saddle River, NJ, 2012, Hueste, M. B. D., Chompreda, P., Trejo, D., Cline, D. B. H., Keating, P. B., "Mechanical Properties of High-Strength Concrete for Prestressed Members", ACI Structural Journal, V. 101, No. 4, July-August 2004. Therefore, the modulus of rupture of the specimens was determined by multiplying the cored specimen split cylinder tensile strength by 1.3 [i.e., 0.87 x 1.5 = 1.3]. These values of f_r were found to correspond to and for the compressive strengths of the rebar and WWR specimens, respectively, which are in the lower range of experimental values for high strength concrete (HSC). Tests of HSC for different curing conditions (1-day heat-cured, 7-day moist-cured, and continuous moist-cured) have demonstrated significant reduction in modulus of rupture with reduced curing timesLogan, A., Choi, W., Mirmiran, A., Rizkalla, S., Zia, P., "Short-Term Mechanical Properties of High-Strength Concrete", ACI Materials Journal, V. 106, No. 5, September-October 2009. 1-day heat-cured specimens, which matches the curing condition of the CSUS specimens, show modulus of rupture values very close to the ACI 318 value, significantly lower than continuously moist cured specimens. This is attributed to the lower permeability of HSC causing differential drying shrinkage strains through the member depth because moisture cannot escape as readily as surface moisture can.

In order to measure the concrete modulus of elasticity (Ec), the 4"x8" cylinders that were cast with the specimens were ~~used~~tested in accordance with ASTM procedure. Although these were not cores from the specimen nor controlled under the same conditions as the specimen, they were considered useful in determining reasonable values of Ec. Compressive stress-strain plots were generated for the cylinders tested, and Ec was determined based on the initial slope of the curves. Compressive strength for these original specimen cylinders was measured as well, and the values of f'c were similar to those measured from the cored samples for each specimen. Therefore, an average value of f'c for all cylinders (cast with specimen and cores) was used for pretest predictions. The concrete properties (f'c, fr, and Ec) used for post-test analysis are summarized in Table 3.

The values of E_c from tests on the original specimen cylinders appear to be relatively low compared to published equations for E_c. These values were compared to an experimental equation for high strength concrete (Equation 1) from Carrasquillo et al. This equation was chosen for accuracy based on Reference French, C. E., "Validation of Prestressed Concrete I-Beam Deflection and Camber Estimates", Research Project, Minnesota Department of Transportation, MN, 2012, which compared various methods of calculating modulus of elasticity. The average concrete strength from Table 3 was used in this equation. Table 4 compares the predicted values from this equation to actual values from the tests. Test values are approximately 33% less than values from approximate equations from the literature. This lower E_c value is due in part to the SCC mix used, and it may also be related to the aggregate stiffnessLogan, A., Choi, W., Mirmiran, A., Rizkalla, S., Zia, P., "Short-Term Mechanical Properties of High-Strength Concrete", ACI Materials Journal, V. 106, No. 5, September-October 2009.

where: f'_c is concrete compressive strength in ksi, and w is the concrete unit weight in pcf.

Table 3 - Concrete Properties Used in Pre-Test Predictions

Sample	f'_c (ksi)	f_r (psi)	E_c (ksi)
Rebar	13.38	865	3920
WWR	12.92	902	4078

Table 4 - Comparison of Actual to Predicted Values of Modulus of Elasticity of Concrete

Sample	E_c (ksi) Actual (Original Cylinders)	E_c (ksi) Predicted (Equation 1)	Ratio (Actual/Predicted)
Rebar	3920	5980	0.66
WWR	4078	5895	0.69

REBAR AND WWR PROPERTIES AND TESTING

Very little information was known regarding the #4 rebar and D20 wire used on the top flange of the specimens. Rebar data could not be traced because it was from a lot that was left over from various jobs. Data on the WWR also could not be traced. The research team decided to salvage steel samples of rebar and WWR from the specimen and test them to get reasonably accurate values of tensile yield strength (f_y) and ultimate strength (f_u), for post-test analysis. 3 rebar samples were taken from the bottom flange of the specimen, which was not affected during the tests. 4 WWR samples were taken from the web of the specimen. Even though the web cracked during all tests, the WWR was not expected to have yielded.

The specimens were tensile tested and strain was recorded up to 0.1 in/in (10%). Stress-strain curves were generated for each tested sample, and yield strength and ultimate strength values were acquired. The stress-strain curve for one of the rebar samples in shown in Figure 10.

This curve is typical, with a clearly defined yield plateau, followed by strain hardening. The stress strain curve for one of the wire specimens is shown in Figure 11, showing no yield plateau. The yield point for the wire specimen is taken as the intersection of the stress-strain curve with the line of 0.0035 in/in strain, per ACI 318-11Error: Reference source not found Sections 3.5.3.4, 3.5.3.5, and 3.5.3.6. The ultimate strength is the highest point in the graph. Table 5 below summarizes the average values of yield strength and ultimate strength for each specimen. These values were used in pretest predictions.

Table 5 - Values of Tensile Yield and Ultimate Strength for #4 Rebar and D20 Wire

Sample	Average f_y (ksi)	Average f_u (ksi)
#4 Rebar	71.0	95.0
D20 Wire	83.0	105.0

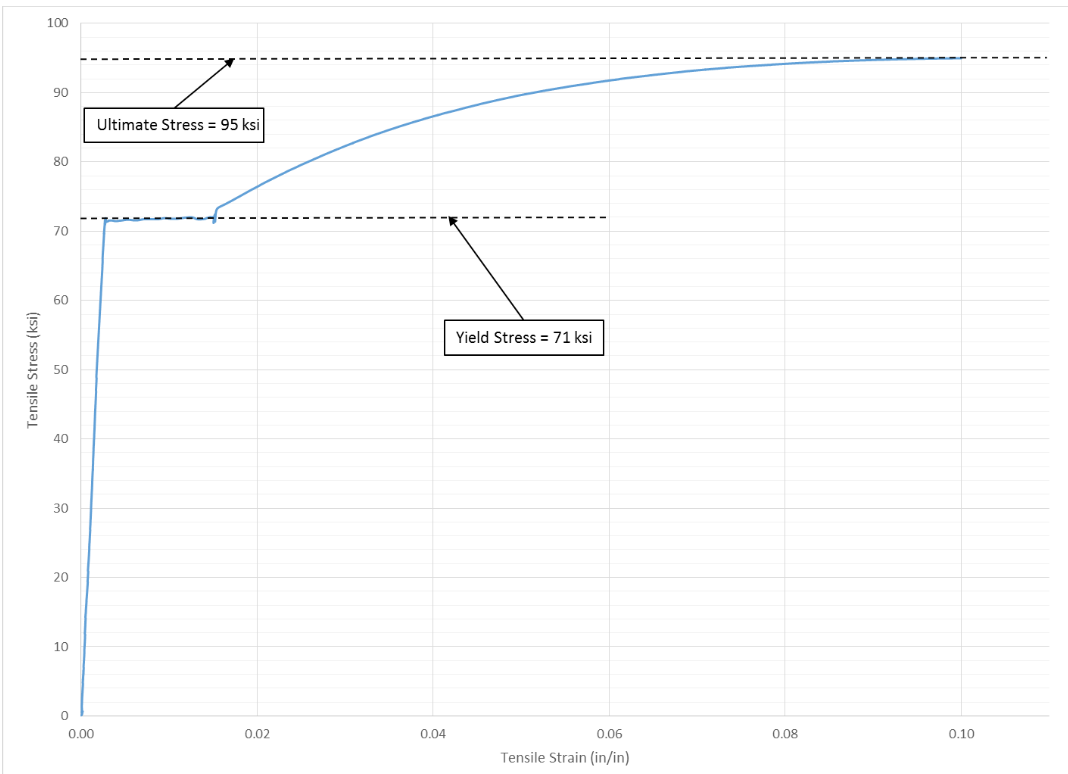

Figure 10 - Tensile Stress vs Tensile Strain Curve for #4 Rebar Specimen R2

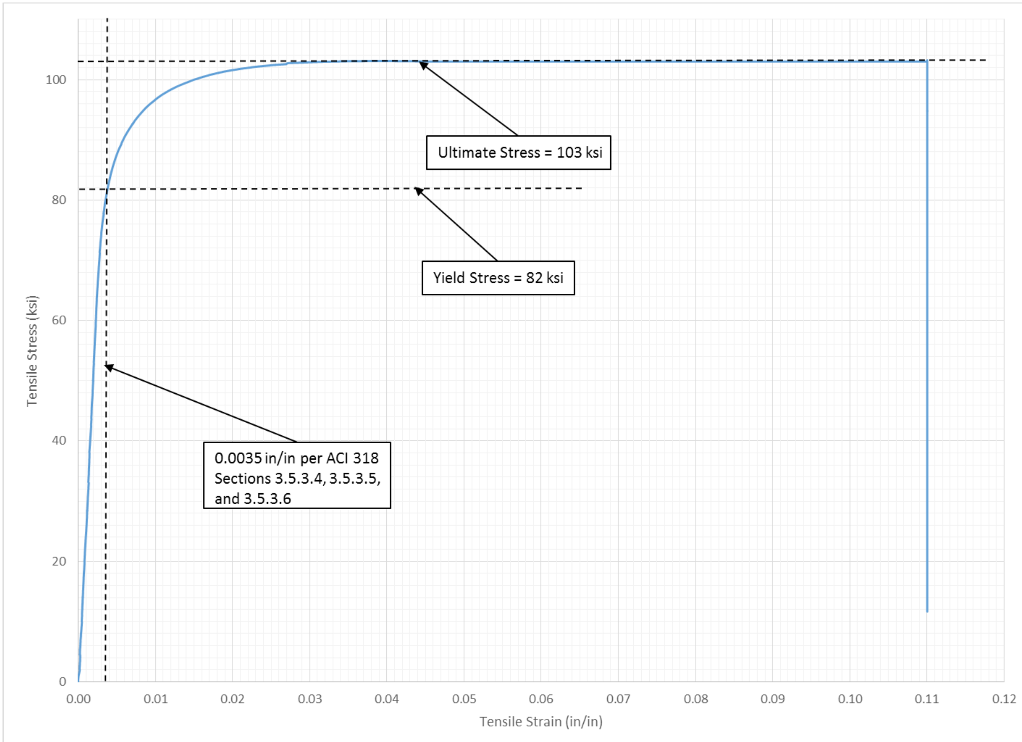

Figure *11* - Tensile Stress vs Tensile Strain Curve for D20 Wire Specimen

TEST RESULTS AND ANALYSIS

TEST R1.5

As shown in Figure 13 and Figure 14, the flange of the R1.5 specimen experienced a flexural failure, characterized by crushing of the underside of the top flange after yielding of the flange flexural reinforcement. The top surface of the flange cracked in flexure at 15.8 kips [Figure 12], followed by rebar yielding at 33.3 kips. The specimen ultimately failed by concrete crushing at the bottom face of the flange at 34.5 kips. A displacement ductility of approximately 2.3 was achieved. This displacement ductility is calculated from R1.5A, the retesting of R1.5 to failure. R1.5 had a displacement ductility of approximately 2.1. The stages of response are summarized graphically in Figure 15 below, showing the applied load versus flange tip deflection.

Figure 12 - R1.5 Test Progress Photo after Initial Cracking

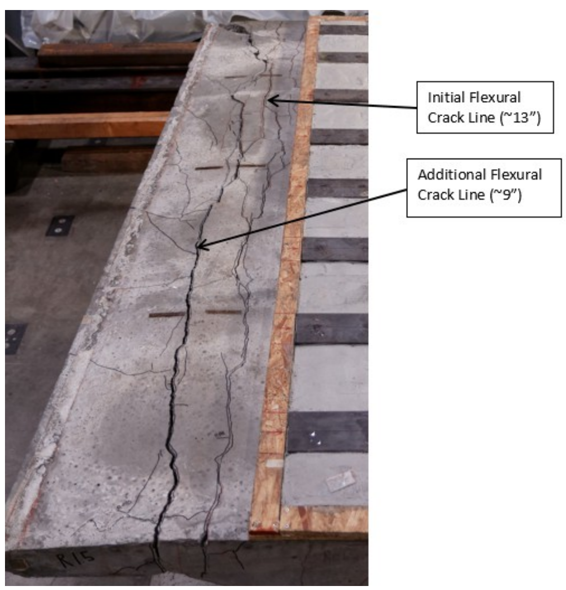

Figure 13 - R1.5A - Post-Test Cracks along Top Surface of Flange

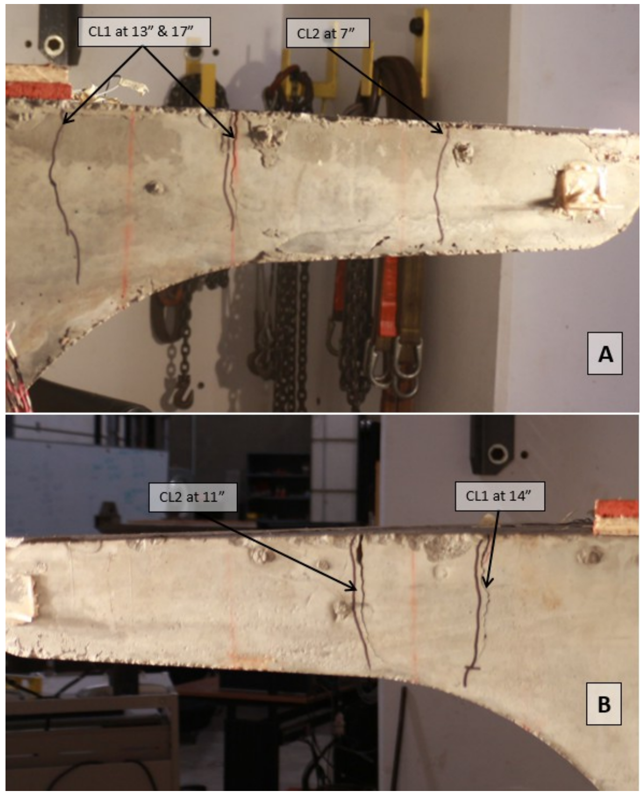

Figure 14 - R1.5 - Post-Test Cracks at Specimen Ends: A) South Side, B) North Side

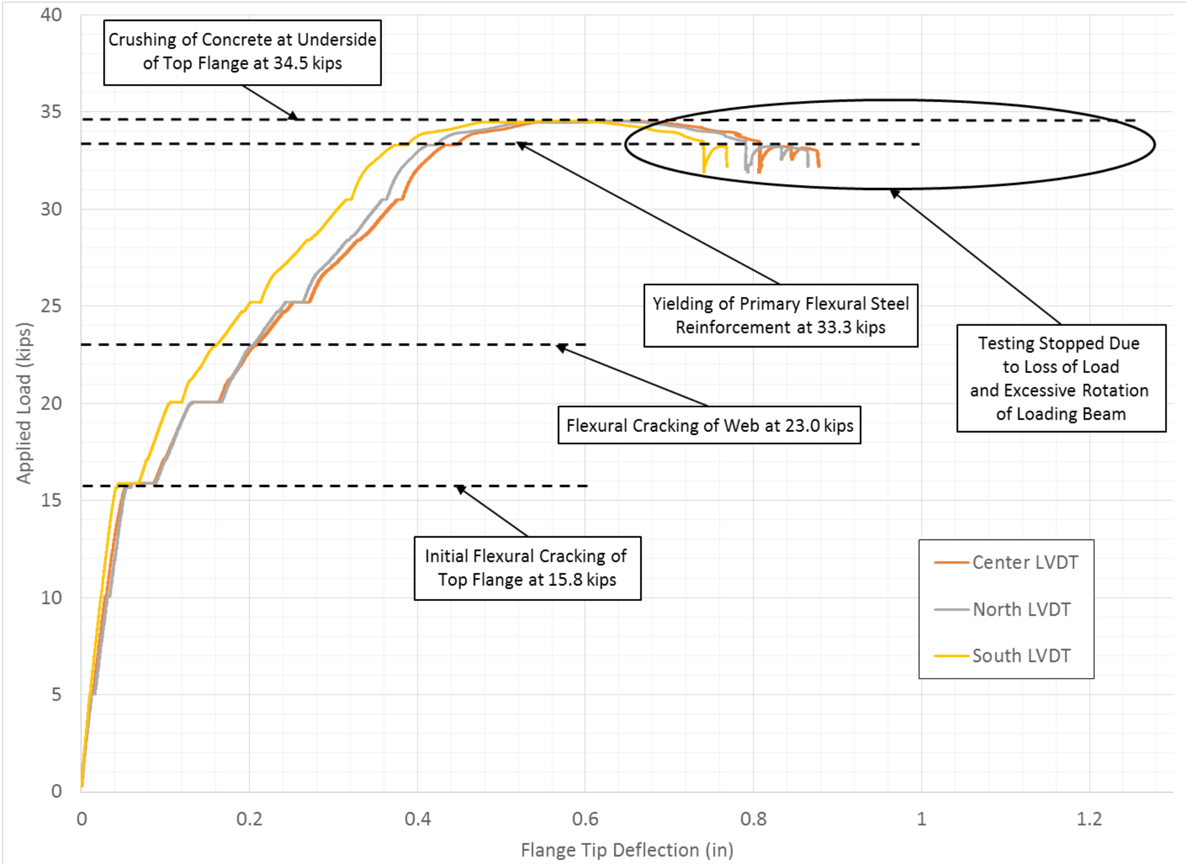

Figure 15 - R1.5 - Applied Load vs Flange Tip Deflection

TEST R2.5

The flange of the R2.5 specimen experienced a flexural-shear failure [Figure 16], characterized by diagonal cracks along the specimen ends and crushing of the underside of the top flange after yielding of the flange flexural reinforcement. First, the top surface of the flange cracked in flexure at 19.0 kips, followed by development of diagonal tension cracks. The rebar yielded at 34.6 kips. The specimen ultimately failed by concrete crushing at the bottom face, due to both flexural and diagonal tension cracks, after reaching 40 kips. The uniform crushing of the bottom of the flange indicates that failure was dominated by flexural crushing, rather than shear. A displacement ductility of approximately 3.0 was achieved. The stages of response are summarized in Figure 17 and Figure 18 below. The development of both flexural and shear cracks is depicted in these figures, along with the corresponding load.

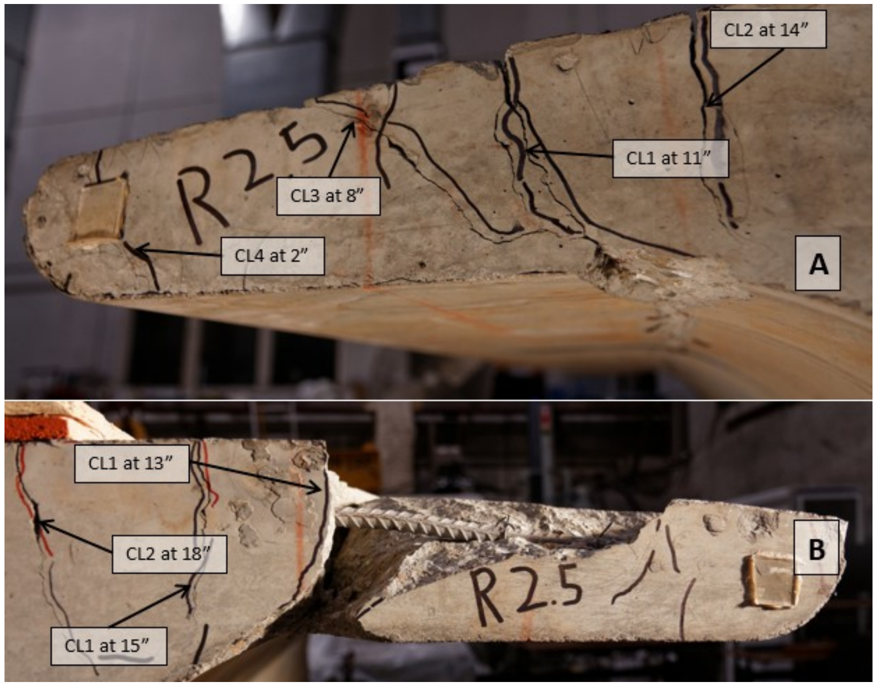

Figure 16 - R2.5 - Post-Test Cracks at Specimen Ends: A) North Side, B) South Side

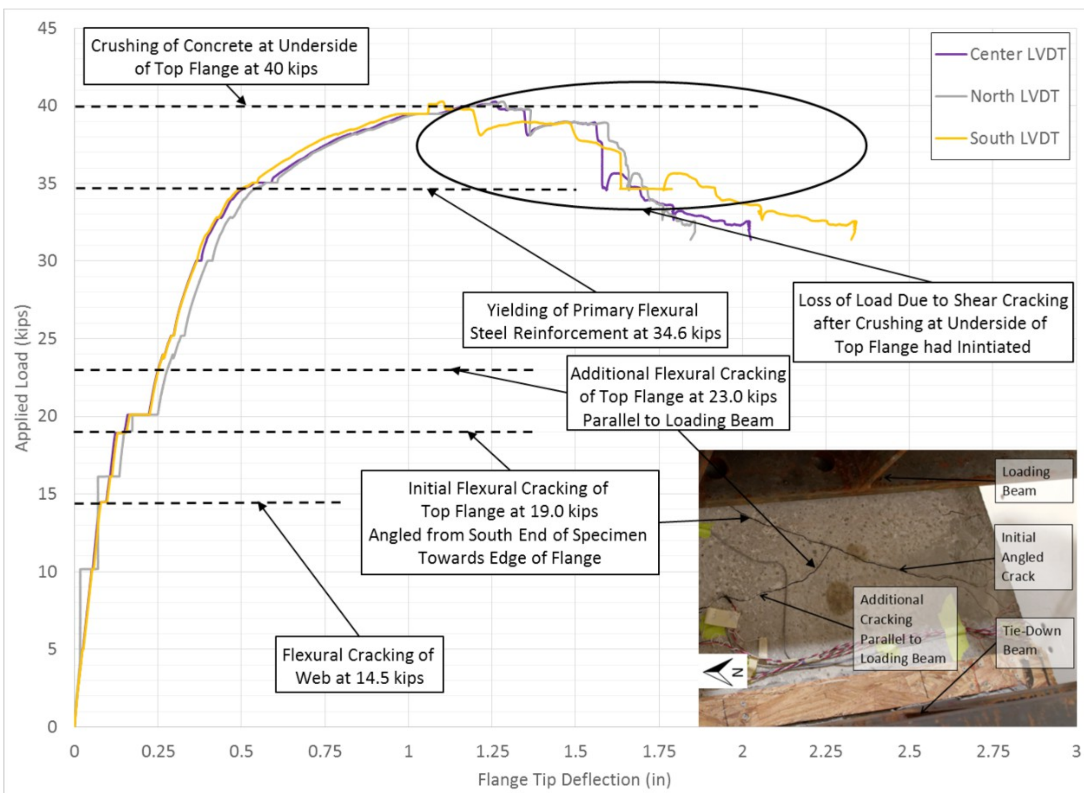

Figure 17 - R2.5 - Applied Load vs Flange Tip Deflection

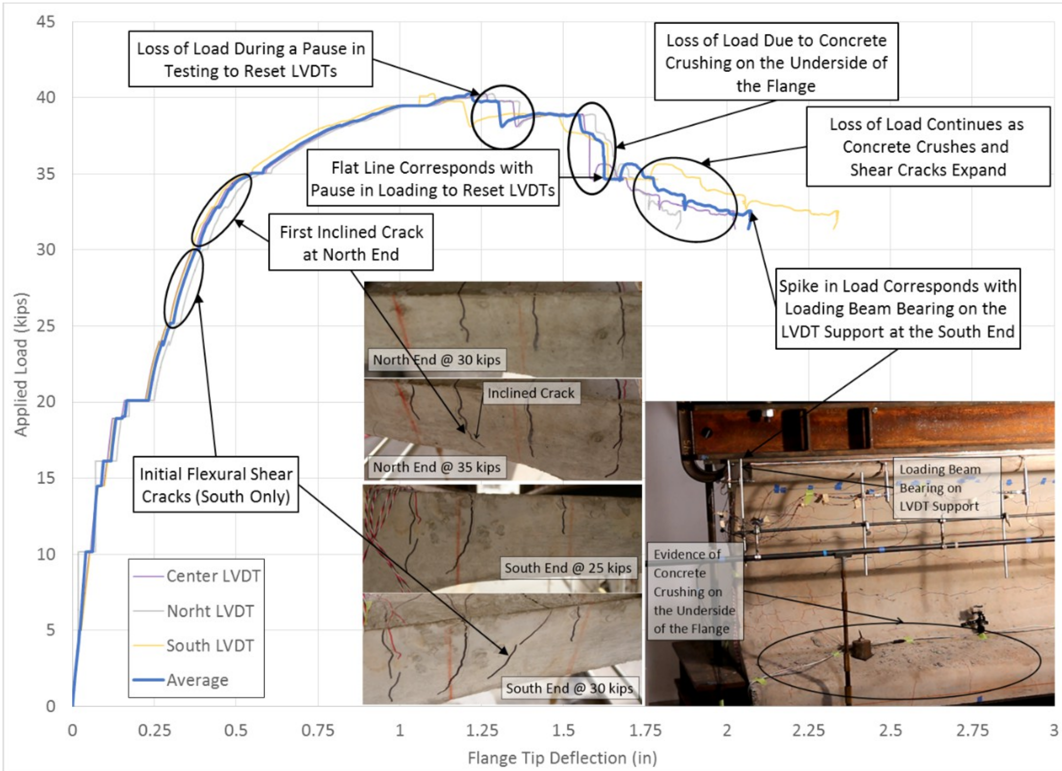

Figure *18* - R2.5 - Applied Load vs Flange Tip Deflection (including failure stages)

TEST W1.5

As shown in Figure 19 the flange of the W1.5 specimen experienced a flexural-shear failure, characterized by diagonal cracks along the specimen ends after yielding of the flexural reinforcement. First, the top surface of the flange cracked in flexure at 15.1 kips, and then the rebar yielded at 36.0 kips. The specimen ultimately failed in an essentially brittle shear failure at 39.1 kips, without any prior indication of diagonal tension cracks. A displacement ductility of only 1.2 was achieved. The stages of response are summarized in Figure 20 below.

Figure 19 - W1.5 - Post-Test Cracks at Specimen Ends: A) North Side, B) South Side

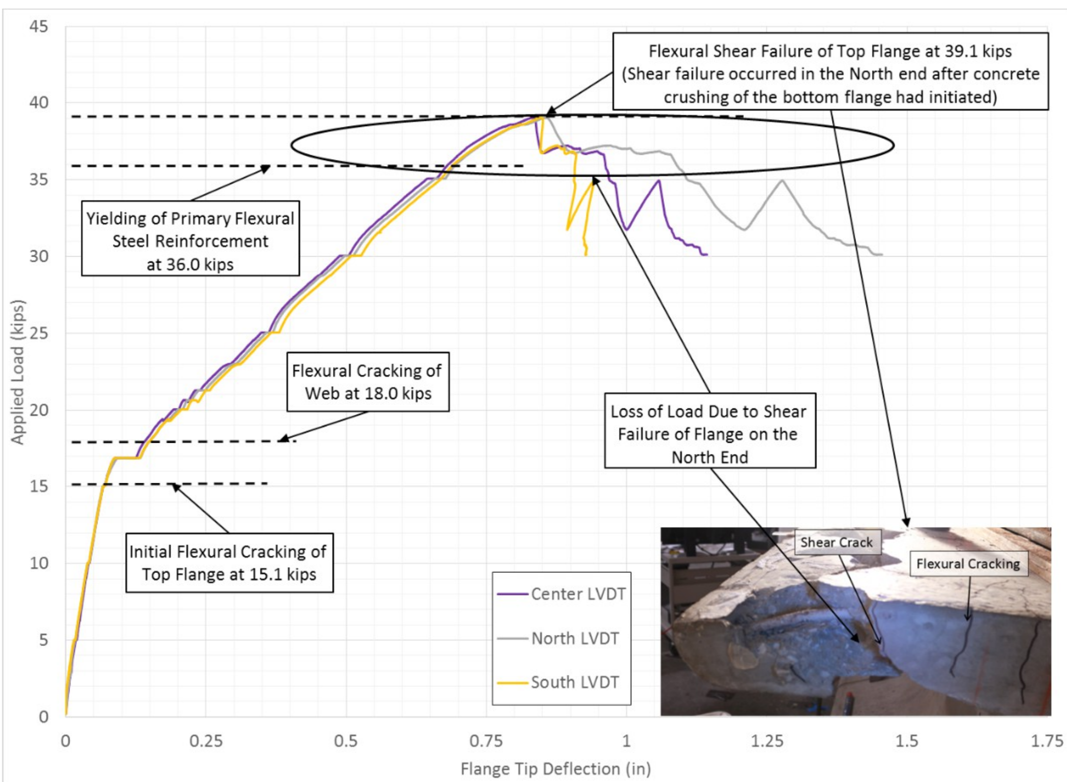

Figure 20 - W1.5 - Applied Load vs Flange Tip Deflection

TEST W0.75

The flange of the W0.75 specimen experienced a flexural-shear failure [Figure 21 and Figure 22], characterized by diagonal cracks along the specimen ends after yielding of the flexural reinforcement. First, the top surface of the flange cracked in flexure at 14.5 kips, and then the rebar yielded at 31.0 kips. The specimen ultimately failed in an essentially brittle shear failure at 34.9 kips, however some diagonal cracks developed prior to that load. The goal of this test was to explore the possibilities of a brittle failure of the tip of the flange. Even though a local shear failure was developed at the tip of the flange, it occurred after the peak load was reached and it did not govern the response of the specimen. A displacement ductility of only 1.4 was achieved. The stages of response are summarized in Figure 23 below.

Figure 21 - W0.75 - First Inclined Cracks at Specimen Ends: A) North Side, B) South Side

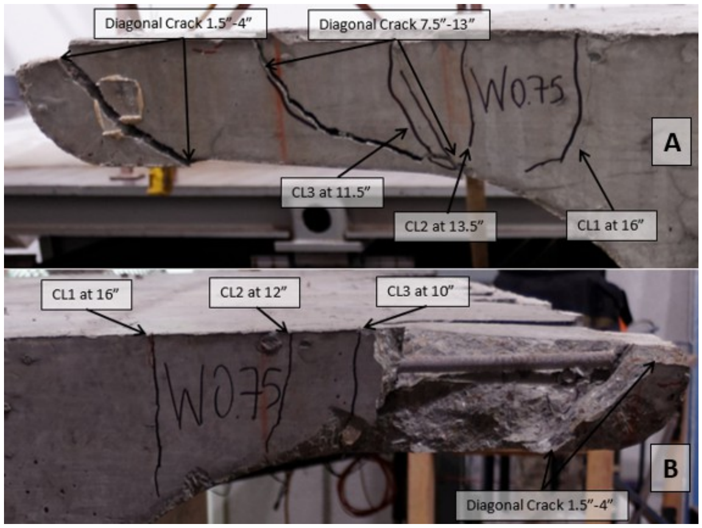

Figure 22 - W0.75 - Post-Test Cracks at Specimen Ends: A) North Side, B) South Side

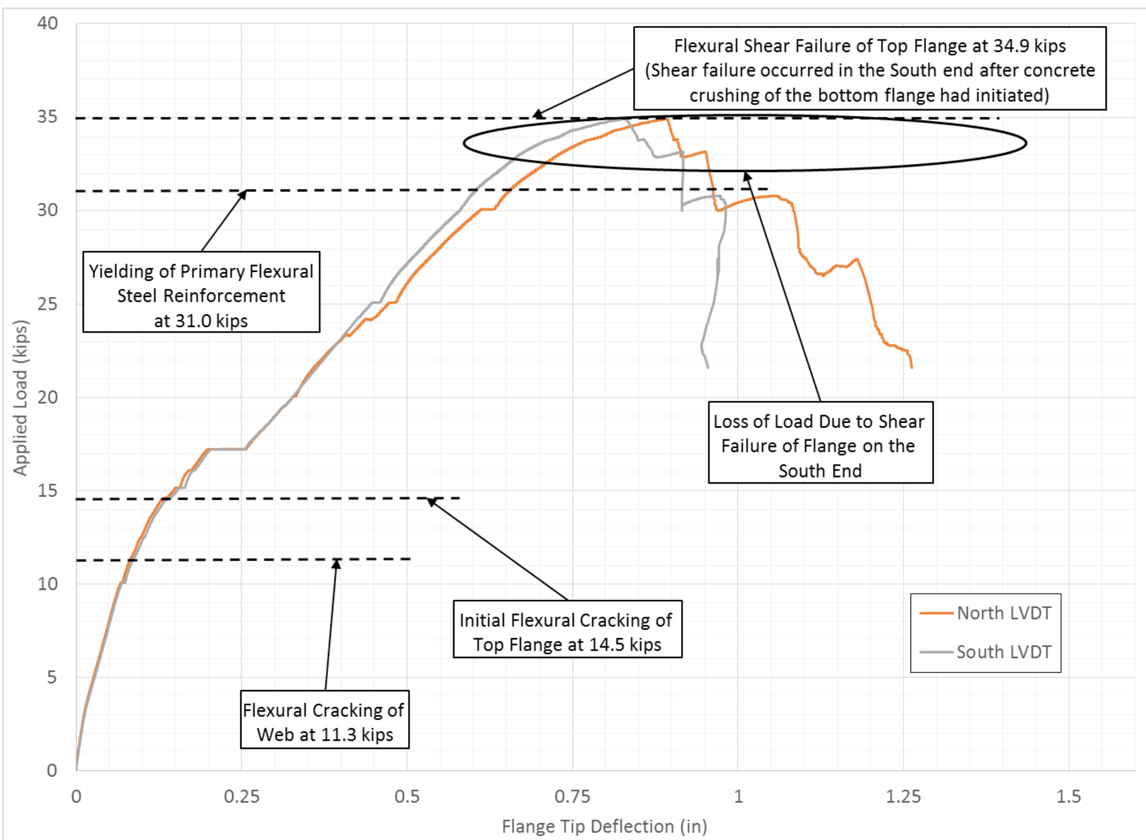

Figure 23 - W0.75 - Applied Load vs Flange Tip Deflection

COMPARISON OF ALL TESTS

A graph depicting the load vs deflection plot for all four tests is shown in Figure 24. The average deflection of the front LVDTs is shown for each test. Test R1.5A is included as well, for purpose of showing ultimate deflection of Test R1.5. Table 6 summarizes the response of all four tests, including cracking load, yield load, ultimate load and failure mode, and maximum deflection with displacement ductility.

R1.5 experienced flexural failure, with the steel yielding extensively before the bottom face of the flange crushed in compression; a displacement ductility of 2.3 was achieved. R2.5 experienced a flexural shear failure, after extensive yielding of the flexural reinforcement, ultimately failing in compression of the bottom flange due to both flexural and shear cracks. This test achieved a displacement ductility of approximately 3.0. In comparison, both sides of the WWR specimen experienced flexural-shear failures, with the steel yielding followed by shear failure shortly after. W1.5 and W0.75 achieved displacement ductility of 1.2 and 1.5, respectively. The failure for these specimens was more brittle, which can be seen from the drops in the load-deflection plot after the maximum load is reached. The brittle failure is consistent with the lower displacement ductility, compared to the R specimens.

When comparing the two baseline tests, R1.5 and W1.5, the WWR specimen had higher load carrying capacity in terms of yielding and ultimate, but cracked at a slightly lower load. The cracking loads are within 5%, which is expected from the almost identical concrete properties between the specimens. The difference in yielding loads (7%), which is less than expected (15%), is mainly due to the higher strength of the D20 wire compared to the #4 rebar. This factor also affects the difference in ultimate load carried by the specimens (12%), despite the different failure modes. Considering the deflection response, the rebar specimen had a larger deflection at ultimate, and showed a much more ductile response overall. In comparison, the WWR specimen, had a lower maximum deflection, and experienced a sudden brittle failure. Therefore, the response of the rebar specimen, despite the lower load carrying capacity, is the more desirable failure mode mainly due to the large displacement ductility.

The two rebar specimens, R1.5 and R2.5, displayed ample ductility. R1.5 experienced flexural failure; R2.5 developed flexural and diagonal tension cracks, but failed in a ductile manner by concrete crushing on the bottom side of the flange. R2.5 carried a higher load at all stages, and also displayed a larger displacement ductility. R2.5 would be the more desirable failure mode given the higher load carrying capacity and larger displacement, hence a better bearing location for the PDP. However, R1.5 would also be a suitable bearing location. In comparison, the response between the two WWR specimens was almost identical, with the W0.75 curve constantly lower than the W1.5. Both tests experienced a flexural shear failure in a brittle manner, seen as a spike in the load-deflection plot. The maximum deflection of both tests was almost identical, with neither test displaying a notable displacement ductility. Given the sudden failure, neither of these tests displayed a desired failure mode. However, under expected loads, failure would not be reached for either test.

In general, the failure of the specimens is consistent with the response of the reinforcing steel in the top flange. The rebar tests, R1.5 and R2.5, show a clear yield plateau, where the steel yields, as well as a lower tensile strength than that for WWR (see stress-strain curves for rebar and WWR, Figure 10 and Figure 11, respectively). The WWR tests, W1.5 and W0.75, show a slight softening on the load-deflection plot, rather than a yielding plateau. It is important to note that the shear failure of these specimens is induced by the higher strength of the WWR flexural reinforcement achieved in testing before significant yield.

As shown by the ratios in Table 7, the actual response was within 36% of the predicted response for all stages. Notably, the predicted cracking load was largely and consistently overestimated for all tests. This is an important consideration for design line loads, which are intended to prevent cracking in field applications of PDPs with the WFG. Potential reasons for this significant difference include:

1) Different exposure conditions between the cores (used to determine the tensile strength) taken from the bottom flange of the specimen and the top flange concrete
2) Possible concrete settlement due to the tendency for aggregates in SCC to settle toward the bottom flange, producing nonhomogeneous concrete with higher strength near the bottom (where the cores were taken)
3) Inherent variability in tensile strength
4) Possible shift of the center of bearing as the camber strip was squeezed and deformed, which could have produced a slightly longer moment arm

The yield load was reasonably estimated for all test, however, the actual response was usually larger than the prediction. One contributor to this difference is due to the calculation being based on a 12" strip of the girder, and not the full length of the specimen of 8.5ft. Since the reinforcement was spaced at 12", the model used for the calculations assumed one bar for the 12" section. This assumption resulted in reinforcement ratio for the model being about 7% less than the actual 8.5ft specimen. Reasons for the minor differences in yield and ultimate load are provided in Reference Gjongecaj, A., "Top Flange Failure Modes for California Wide Flange Girder using Rebar and Welded Wire Details", Thesis, California State University, Sacramento, CA, 2014..

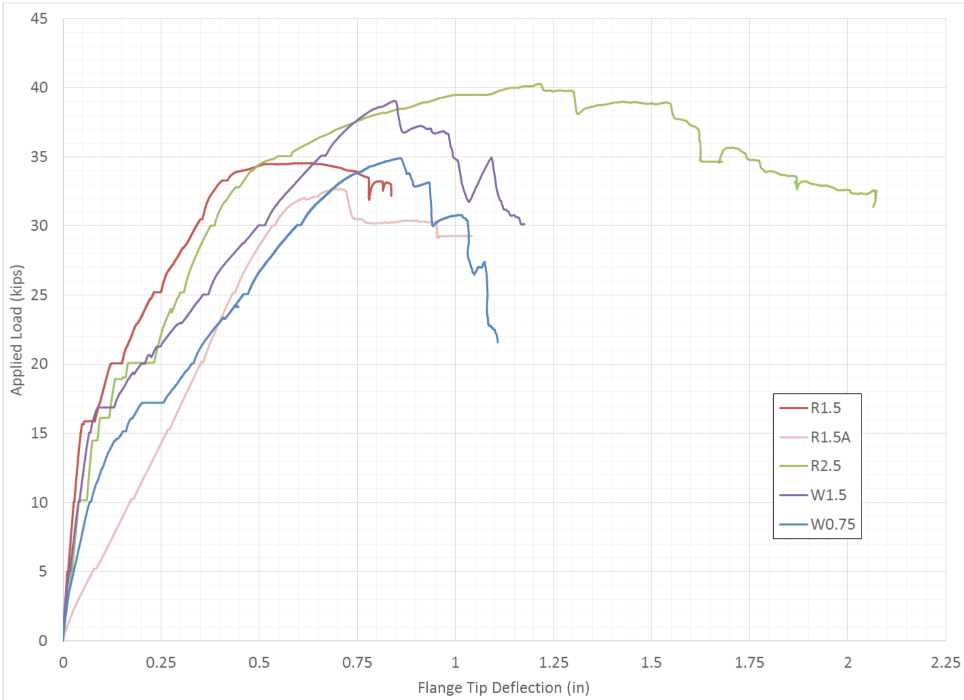

Figure 24 - Applied Load vs Flange Tip Deflection (All Tests)

Table 6 - Summary of Response for All Four Tests

Test ID	Initial Flexural Cracking of Top Flange	Yielding of Primary Flexural Reinforcement	Ultimate Load (Failure Mode)	Maximum Deflection (Displacement Ductility)
R1.5	15.8 kips	33.3 kips	34.5 kips (Flexure)	0.953 in* (2.3)*
W1.5	15.1 kips	36.0 kips	39.1 kips (Flexure-Shear)	0.849 in (1.2)
R2.5	14.5 kips	34.6 kips	40.0 kips (Shear)	1.550 in (3.0)
W0.75	14.5 kips	31.0 kips	34.9 kips (Shear)	0.863 in (1.4)

*From Test R1.5A

Table 7 - Comparison of Actual to Predicted Loads for All Specimen

Stage of Response	R1.5 - Ratio Actual/Predicted	R2.5 - Ratio Actual/Predicted	W1.5 - Ratio Actual/Predicted	W0.75 - Ratio Actual/Predicted
Initial Flexural Cracking of Flange	0.69	0.76	0.64	0.65
Yielding of Flange Reinforcement	1.18	1.11	1.09	1.00

Flexural Shear Failure	N/A	N/A	1.09	0.87
Concrete Crushing in Flexure	0.93	0.96	N/A	N/A

CONCLUSIONS

Based on test results and analysis for the four WFG flange specimens, the following conclusions are made:

- Flexural cracking of the top flange of the WFG is not expected under typical construction loads.
- The expected location of initial flexural cracking is at the maximum flexural stress location, a significant distance away from the PDP-supporting camber strip; shear cracks are not expected to precede initial flexural cracking.
- A ductile or brittle failure mode may develop at the failure load, depending on flange detailing, PDP bearing location, and actual material properties.
- Top flanges using WWR details that match the flexural reinforcement area of rebar details (e.g., D20 wire vs. #4 rebar) are more likely to exhibit a brittle failure under expected PDP bearing locations, if overloaded to ultimate; this is due to the typically higher tensile strength and non-linear stress-strain characteristics of WWR compared to those for Grade 60 rebar.
- Conventional concrete mechanics can be used to reasonably determine the key stages of top flange flexural and shear cracking and failure.
- Other factors such as girder prestressing, pre-existing cracks, 3-D effects, and field conditions not accounted for in this test program may affect the initial flexural load in practice; however, the use of an appropriate safety factor in establishing a maximum line load for design (construction) should reasonably account for these uncertainties.
- Test results provide a sufficient basis for improved detailing, including side cover over top flange flexural reinforcement and minimum and maximum edge distances for PDP camber strip locations.
- An FEM model is being considered for future research.

RECOMMENDATIONS

Based on test results and conclusions, the following are recommended for implementation of PDPs on WFGs using the polystyrene (camber strip) support system:

- Minimum end cover for top flange transverse reinforcement (to side face of girder) should be 1.0 in. In addition, maximum end cover for this reinforcement should be 1.5 in. Minimum top cover for this reinforcement should be 1.0 in [see Figure 25]. Placement tolerance for this reinforcement should not exceed +/- 0.5 in and should be shown in the contract documents. No special tolerances are specified for the Wide Flange Girder.

- Minimum side cover for top flange longitudinal reinforcement placed at the tip of the flange should be 1.0 in.
- Minimum clear edge distance for polystyrene camber strips placed on the top flange should be 1.5 in. A maximum clear edge distance for polystyrene camber strips of 2.0 in is recommended.
- A camber strip cross section using a width to height ratio of at least 1.0 is recommended for typical applications.

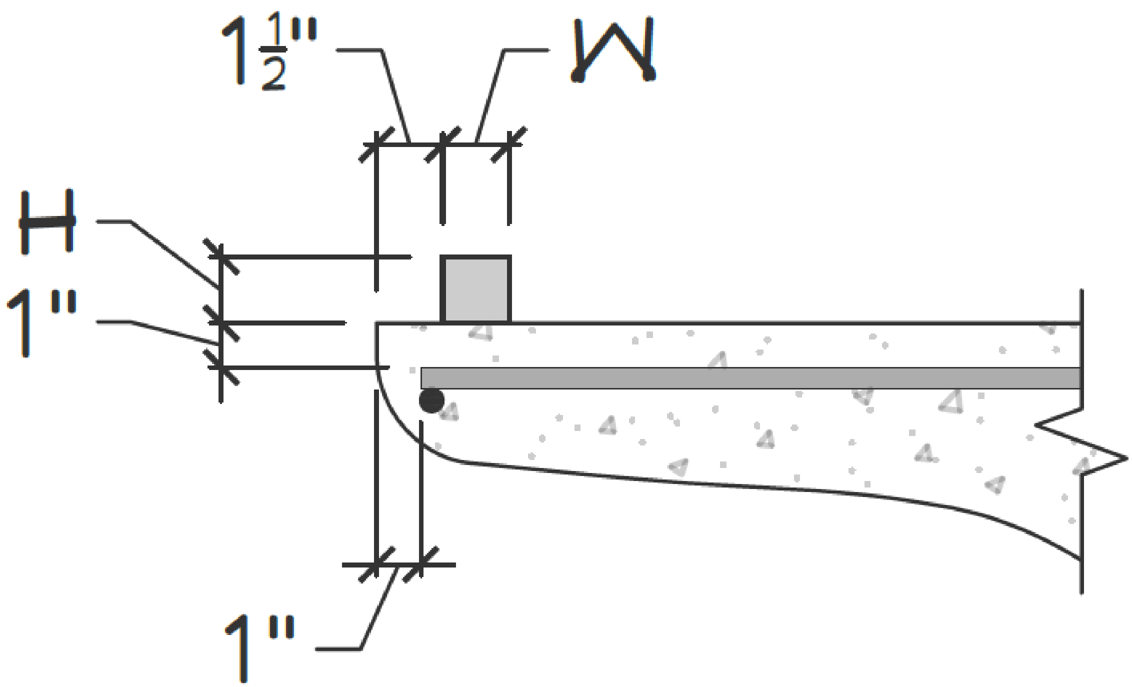

Figure 25 - Proposed WFG top flange detailing

Based on test results, representative design line loads (maximum uniform load in kip/ft applied on girder top flange during construction) for use in practice are shown in Table 8. Design values are intended to prevent initial flexural cracking due to non-composite action during construction due to factored deck panel self-weight and the maximum of either factored construction live load or factored CIP deck self-weight. Actual test values that caused initial flexural cracking, shown in the first column, are normalized for bearing location in the second column, using 1.5" from the edge as the basis. These values are normalized by the square root of f'c (psi) in the third column. An overall strength reduction factor of 0.70 (i.e., safety factor of 1.4) is then applied for design loads, as shown in the last (fourth) column. This safety factor reflects potential variability in material and sectional properties as well as other factors related to fabrication and construction practices such as combined fabrication and placement tolerances that may reduce the flexural cracking load.

Additionally, even in cases of an unlikely overload, this factor would account for a potential brittle failure mode (applicable when using the WWR detail).

Based on Table 8, a line load value of 0.0109 kip/ft (f'_c in psi) is recommended as a maximum PDP design line load for construction. A factor of safety is reasonably incorporated into the lines loads permissible for construction. The effect of concrete strength is directly accounted for, as shown in Table 8. Similar tables may be developed for common ranges of girder f'_c as well as different material properties and load locations.

Table 8 - Recommended Design Line Load

Test	**Line Load to Cause Flexural Cracking of Flange (kip/ft)**	~~**Lime**~~ **Line Load to Cause Flexural Cracking of Flange – Normalized for Bearing Location (kip/ft)**	**Line Load To Cause Flexural Cracking of Flange – Normalized for Concrete Strength (kip/ft) (f'_c in psi)**	**Recommended Design Line Load with 0.7 Strength Reduction Factor (kip/ft) (f'_c in psi)**
R1.5	1.86	1.86	0.0161	0.0113
R2.5	2.24	2.14	0.0185	0.0130
W1.5	1.78	1.78	0.0157	0.0110
W0.75	1.71	1.77	0.0156	0.0109

ACKNOWLEDGEMENTS

The authors would like to acknowledge the following individuals for their contributions to this project:

Jim Ma, P.E. (Bridge Engineer, Caltrans, Second Reader), Say-Gunn Low, Ph.D., P.E., (Bridge Engineer, Caltrans), and Douglas Mooradian (Executive Director of PCI West) for serving as the Industry Advisory Committee.

Con-Fab California Corporation and Brent Koch, P.E. (Chief Engineer) for donating the specimens used for this project.

Professor Ben Fell, P.E., for his assistance in planning and conducting testing.

Laboratory technicians Jim Ster, Mike Newton, and the Tech Shop of the College of Engineering and Computer Science for their help in fabrication and assembly of the test setup.

The following graduate and undergraduate students for their help with this project: Rakeeb Khan (analysis lead), Khanh Nguyen and Jesse Gilbert (analysis), Whitney Maxfield (instrumentation, assembly), Michael Capili (drawings), Michael Lucas (camera, testing), William Cope and Mathew Rosatelli (construction, testing).

REFERENCES

1. Tadros, M. K., "New Developments in Long Span Precast Girder Technology", *14th Annual Caltrans/PCMAC Bridge Seminar Proceedings*, Sacramento, CA, 2007.
2. Geren, L. K., Tadros, M. K., "The NU Precast/Prestressed I-Girders Series", *PCI Journal*, V. 39, No. 3, May-June 1994, pp.26-39.
3. Ma, J., "The New Wide-Flange Girder Family in California: Benefits and Capabilities", *16th Annual Caltrans/PCMAC Bridge Seminar Proceedings*, Sacramento, CA, 2009.
4. Caltrans, *"Bridge Design Aids"*, California Department of Transportation, Sacramento, CA, 2012.
5. Koch, B. R., "*Wide Flange Test For Capacity To Support Deck Panels*", Construction Drawings, ConFab California Corporation, Lathrop, CA, 2014.
6. XS01-180-1e, *"Precast Concrete Deck Panel Polystyrene Support System"*, Draft XS Sheets, State of California Department of Transportation, CA, 2013.
7. Gjongecaj, A., *"Top Flange Failure Modes for California Wide Flange Girder using Rebar and Welded Wire Details"*, Thesis, California State University, Sacramento, CA, 2014.
8. AASHTO, *"AASHTO LRFD Bridge Design Specifications, Customary U.S. Units, 6th Edition"*, American Association of State Highway and Transportation Officials, DC, 2012.
9. Neville, A. M., *"Properties of Concrete"*, Fourth Edition, Pearson Education Inc., Essex, England, 2000.
10. Wight, J. K., MacGregor, J. G., *"Reinforced Concrete Mechanics and Design"*, Sixth Edition, Pearson Education Inc., Upper Saddle River, NJ, 2012.
11. Hueste, M. B. D., Chompreda, P., Trejo, D., Cline, D. B. H., Keating, P. B., "Mechanical Properties of High-Strength Concrete for Prestressed Members", *ACI Structural Journal*, V. 101, No. 4, July-August 2004, pp. 457-465.
12. Logan, A., Choi, W., Mirmiran, A., Rizkalla, S., Zia, P., "Short-Term Mechanical Properties of High-Strength Concrete", *ACI Materials Journal*, V. 106, No. 5, September-October 2009, pp. 413-419.
13. French, C. E., *"Validation of Prestressed Concrete I-Beam Deflection and Camber Estimates"*, Research Project, Minnesota Department of Transportation, MN, 2012.
14. ACI 318-11, *"Building Code Requirements for Structural Concrete (ACI 318-11) and Commentary"*, ACI Standard, American Concrete Institute, Farmington Hills, MI, 2011.